Yu-Long Zhao, Teng-Jiang Hu*, Xiu-Yuan Li, Zhuang-De Jiang, Wei Ren and Ying-Wei Bai

Design and Characterization of a Large Displacement Electro-thermal Actuator for a New Kind of Safety-and-Arming Device

Abstract: The design, fabrication and characterization of a distinctive electro-thermal MEMS safety-and-arming device are presented in this paper. The device is comprised of a V-shape actuator and a micro lever. The V-shape actuator can generate a large output force but small displacement; thus, it is necessary to design a micro lever to amplify the insufficient displacement, which can broaden the device applications in different fields. The temperature distribution, the maximum displacement and the step response time of the actuator are analyzed and validated by the finite element analysis software ANSYS. The whole device is fabricated on SOI (Silicon-on-Insulator) wafer, and MUMPs process is introduced. The characterized performance of the device shows output displacement at more than 150 μm within 17 V driving voltage, and the consuming power is about 1.53 W. The chip size is about $5 \times 5 \times 0.5$ mm^3, which can be easily integrated with other micro devices.

Keywords: MEMS, electro-thermal actuator, safety-and-arming device, micro lever

DOI 10.1515/ehs-2014-0037

Introduction

The miniaturization of the safety-and-arming (SA) device contributes a lot to the weapon supporting systems (Lake et al. 2010; Robinson, Wood, and Hoang 2005; Zunino III et al. 2008), in the sense that smaller size can provide additional space for sensors and power arrangements (Donald et al. 2001; Robinson 2003). Micro-Electro-Mechanical-System (MEMS) has a great potential to meet the demands.

According to different principles, MEMS actuators mainly fall into four classes (Dong et al. 2003; Jay et al. 2011): electrostatic, piezoelectric, electro-thermal, and electromagnetic. Electrostatic actuators possess less functional robustness and small range of controllable displacement. Electromagnetic and piezoelectric actuators may require some special materials which will complicate the fabrication process. Electro-thermal actuators can generate a stable and controllable displacement, a large force, and have the compatibility with standard IC fabrication process and materials. Thus, they are widely used in many different applications.

Herein, we present a silicon SA device with electro-thermal actuator and micro lever, which is highly desirable to accommodate the aforementioned competing requirements in miniaturization, low cost, easily integrated. The whole mechanism is fabricated on a SOI wafer utilizing Multiuser-MEMS-Process (MUMPs) (Jay et al. 2011; Ostrow II, Lake, and Lombardi III 2012).

Device Structure and Modeling

The electric current passes through the electro-thermal actuator can generate relevant heat. The fundamental equation to describe the three dimensional heat transfer problem is listed below (De Dobbelaere et al. 2002).

$$\nabla^2 T + \frac{q}{k} = \frac{1}{\alpha}\frac{\partial T}{\partial t} \quad [1]$$

where $\nabla^2 T = \partial^2 T/\partial x^2 + \partial^2 T/\partial y^2 + \partial^2 T/\partial z^2$ and $\alpha = k/\rho c$. T is temperature distribution, α is known as the thermal diffusivity, k is the thermal conductivity of the material, ρ represents the density, c is the specific heat capacity, and q accounts for the volumetric heat release.

Figure 1 shows the heat transfer path in the electro-thermal actuator. The length of the actuator is much larger than its cross section, thus, the analysis can be seen as the one-dimensional heat diffusion problem, and the basic equation given in eq. [1] can be simplified (Chiorean,

*Corresponding author: Teng-Jiang Hu, State Key Laboratory for Mechanical Manufacturing System, Xi'an Jiaotong University, Xi'an, Shaanxi 710049, China, E-mail: hu.tengjiang@stu.xjtu.edu.cn
Yu-Long Zhao, Xiu-Yuan Li, Zhuang-De Jiang, State Key Laboratory for Mechanical Manufacturing System, Xi'an Jiaotong University, Xi'an, Shaanxi 710049, China
Wei Ren, Ying-Wei Bai, Science and Technology on Applied Physical Chemistry Laboratory, Shaanxi Applied Physical Chemistry Research Institute, Xi'an 710061, China

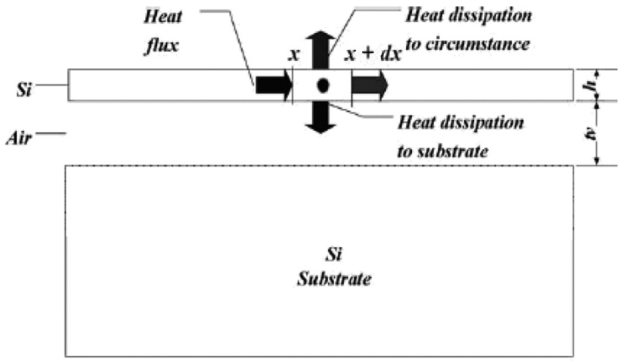

Figure 1: The heat transfer path in actuator.

Dudescu, and Pustan 2014; Enikov, Kedar, and Lazarov 2005). Figure 2 shows the basic structrue of the beam. As a result, the temperature distribution of the beam can be obtained by the following equation:

$$k_s \frac{d^2T(x)}{dx^2} + J^2\rho = \frac{S}{h}\frac{T(x) - T_r}{R_T} \quad [2]$$

With the thermal boundary conditions:

$$T(0) = T(L) = T_r \quad [3]$$

where k_s is the thermal conductivity of silicon. $J = I/wh = V\cos\theta/\rho L$, it represents the density of the electric current. V is the voltage that applied on the actuator. θ is the angle of the beam. ρ is the electrical resistivity of silicon. L means the length of the chevron beam. $R_T = t_V/k_V$, it is the thermal resistivity between the bottom of the structure and the surface of the substrate. It reflects the amount of heat dissipation to substrate. t_v and k_v are the thickness and the thermal conductivity coefficient of the air gap respectively. $S = \frac{h}{w}\left[\frac{2t_V}{h} + 1\right] + 1$, it is the shape factor which accounts for the heat transfer through all sides of a beam (Zhang et al. 2006). T_r is the reference temperature, and usually it equals to the room temperature. The steady temperature distribution of the chevron beam can be expressed as:

$$T(x) = C + De^{Ax} + Ee^{-Ax} \quad [4]$$

$$A^2 = \frac{S}{k_s h R_T} \quad [5]$$

$$B = -\frac{ST_r}{k_s h R_T} - \frac{J^2\rho}{k_s} \quad [6]$$

$$C = -\frac{B}{A^2} = \frac{J^2\rho h R_T + ST_r}{S} \quad [7]$$

$$D = \frac{(T_r - C)(1 - e^{-AL})}{e^{AL} - e^{-AL}} \quad [8]$$

$$E = \frac{(T_r - C)(e^{AL} - 1)}{e^{AL} - e^{-AL}} \quad [9]$$

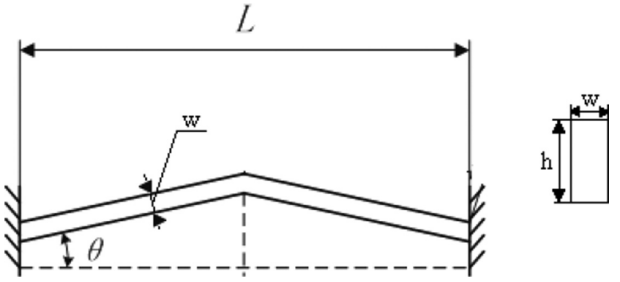

Figure 2: The structure of the V-shape electro-thermal actuator.

Table 1: Basic parameters of the material.

Item	Data	Unit
k_p	141×10^6	pW/(μm.K)
ρ	2×10^{-10}	V.μm/(pA)
T_s	273	K
V	14	V
α	2.6×10^{-6}	K^{-1}
t_v	2	μm
k_v	2.44×10^4	pW/(μm.K)
E	169,000	MPa
u	0.3	

The relevant parameters are shown in Table 1 and the result of analytical modeling is verified with ANSYS. The temperature distribution of the chevron beam is shown in Figures 3 and 4. The two methods show the maximum temperatures of the device are 903.4755 K and 907.349 K respectively, and both of them occur in the middle of the chevron beam.

Thermal expansion is well known for the feature of large output force, but its output displacement is too small to apply directly (Yang et al. 2009). It could not be enough to satisfy the basic requirement of a large displacement. Thus, we introduce a micro lever to magnify the displacement. The micro lever is usually joined by some flexible beams in order to simplify the fabrication. The basic structure of the micro lever is shown in Figure 5. The shorter and wider flexible beam can enhance the stiffness of the whole structure. However, it will reduce the flexibility of the lever and decrease the amplification coefficient.

$$\begin{bmatrix} \frac{l_f}{Etw_f} & 0 & 0 \\ 0 & \frac{l_f^3}{3EI} & \frac{l_f^2}{2EI} \\ 0 & \frac{l_f^2}{2EI} & \frac{l_f}{EI} \end{bmatrix} \begin{bmatrix} F_y \\ 0 \\ F_y l_1 \end{bmatrix} = \begin{bmatrix} \Delta x \\ \Delta y \\ \Delta\alpha \end{bmatrix} \quad [10]$$

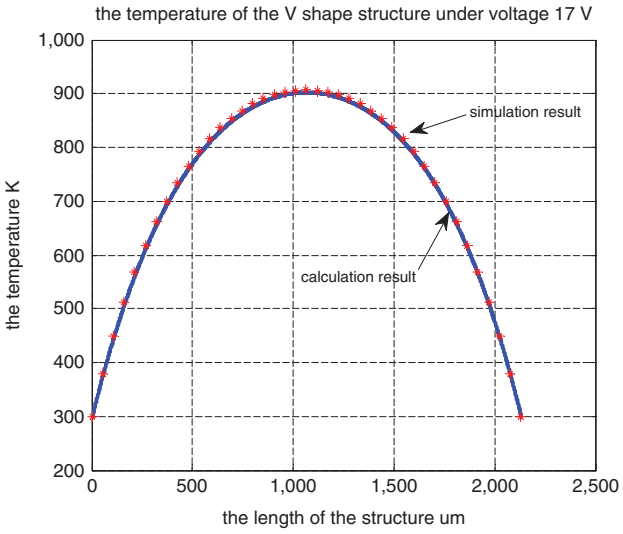

Figure 3: The temperature distribution of the electro-thermal chevron beam. The red star '*' represents the simulation result and the blue line represents the calculation result.

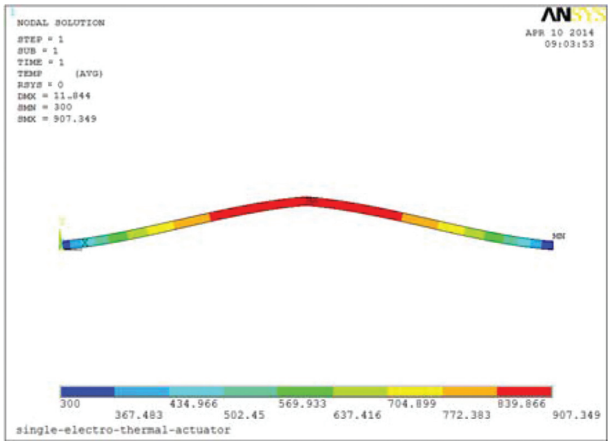

Figure 4: The temperature distribution result of the V-shape electro-thermal actuator given by ANSYS.

The parameter E is the Young's modulus of silicon. l_f and w_f are the length and the width of the flexible beam respectively. $I = tw_f^3/12$, it is the second moment coefficient. t is the thickness of the flexible beam. Under the input force F_y, the final displacement of the micro lever is subjected to $D = (l_1 + l_2)\sin(\Delta\alpha)$.

The comparison between analytical and FEM results is shown in Figure 6. It can be seen clearly that the micro lever has a linear characteristic and has a good ability to enlarge the insufficient displacement of the electro-thermal chevron beam. The finite element analysis is introduced to analyze the whole device, and the result is shown in Figure 7. The maximum displacement with micro lever is

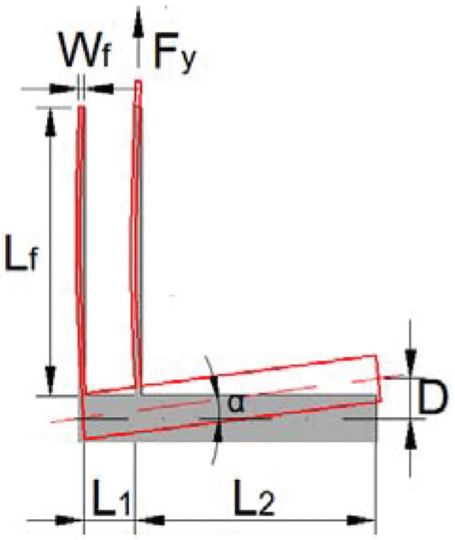

Figure 5: The structure of micro lever.

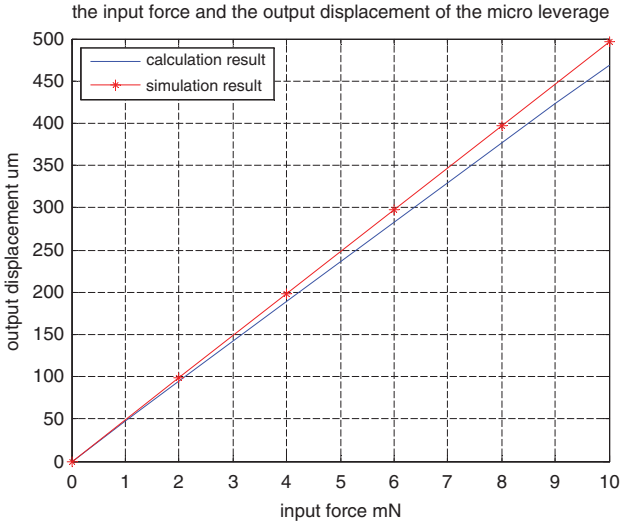

Figure 6: The characteristic of the micro lever.

238.179 μm. Compared to the single electro-thermal chevron beam, the displacement is enlarged about 20 times.

Device Fabrication

The device is fabricated on a silicon-on-insulator (SOI) wafer with a 50 μm device layer of silicon, 3 μm buried layer of silicon dioxide, and handle layer of 430 μm silicon in thickness. The crystal orientation of the device layer and the handle layer is (100). The resistivity of the device layer is 0.01~0.02 Ωcm. The low resistivity can provide a good electrical path of the MEMS device. The fabrication process can be seen in Figure 8. First, bond pads were placed on the surface of the device layer using

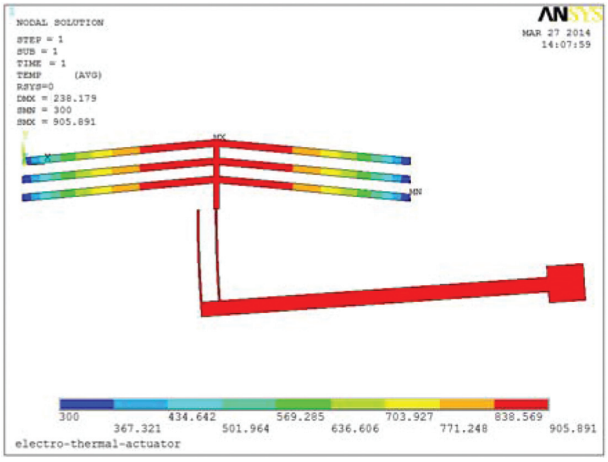

Figure 7: The maximum displacement of the V-shape electro-thermal actuator with micro lever given by ANSYS.

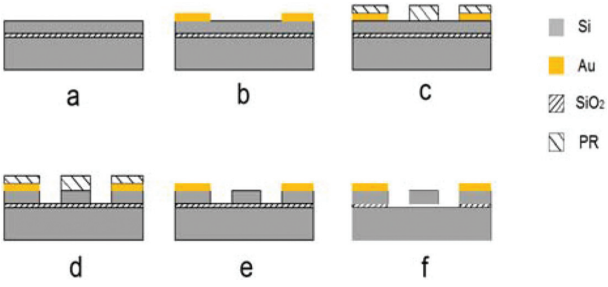

Figure 8: The fabrication process of the device.

lift-off. In order to have a good ohmic contact and stable pad surface for wire bonding, two layer structure of the pad were introduced – Cr/Au in 50 nm/300 nm. Next, the wafer was patterned in photoresist (PR) and etched to the buried oxide layer by the deep reaction ion etching (DRIE). DRIE can create a high aspect ratio of depth and width and provide a vertical sidewall of the structure. A large amount of PR can be removed by acetone after the process, and the remains can be cleaned by oxygen plasma aching. Finally, the whole device was released by etching the buried oxide layer in HF liquid. Figure 9 shows the device after fabrication.

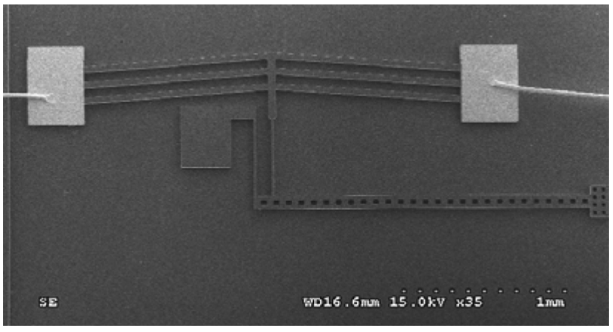

Figure 9: The overview of the device through SEM.

Test and Result

The device we mentioned in this paper works under 20 g acceleration in *y* direction, and the inertia force is about 8.14 μN. Compared to the output force, 190.74 mN, the inertia force can be ignored. In order to simplify the tests, experiments are made under no acceleration in *y* direction. In Figure 10, a step voltage is applied on the device, and the maximum displacement is 178.809 μm. Compared to the analytical and FEM results, which are 240.12 μm and 238.179 μm, the error are 34.3% and 33.74% respectively, shown in Figure 11.

The authors think it is the micro lever which consumes the energy. As a result, the average temperature of the device could be lower than the simulation result. Moreover, some parts of SiO_2 may still remain beneath the movable structure, which can generate fiction force that decreases the deformation.

According to Figure 12, the energy consumption of the device under 17 V is 1.53 W. Figure 13 shows the experiment setup used for measuring the step response time of the electro-thermal beam (Lai, Bordatchev, and Nikumb 2006). The setup is consisted of a signal generator, oscilloscope, resistor and the electro-thermal actuator. The signal generator provides a square signal with 50 ms in period, and the peak and valley values are 10 V and 0 V respectively. The actuator is connected to the signal generator through a 30 Ω resistor. One channel of the oscilloscope is connected to the actuator to measure and record changes

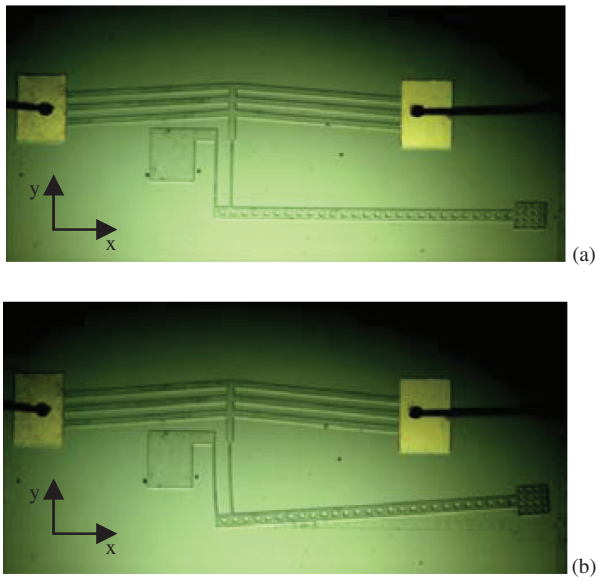

Figure 10: The displacement of the actuator under 0 g in *y* direction. The applied voltage in (a) and (b) are 0 V and 17 V respectively.

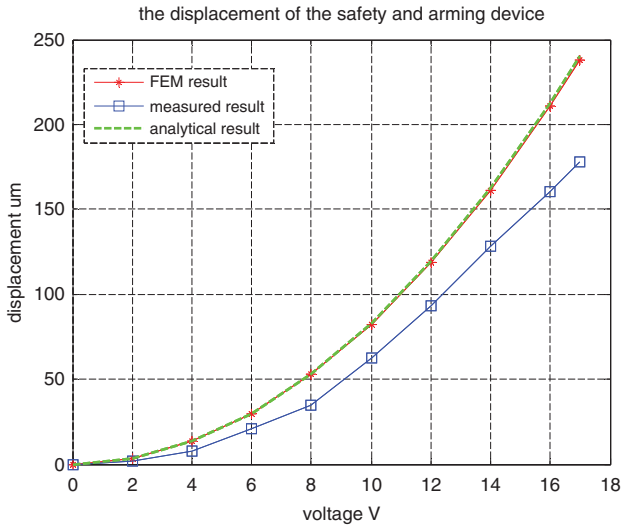

Figure 11: The relationship between the applied voltage and the displacement of the whole device under 0 g in *y* direction.

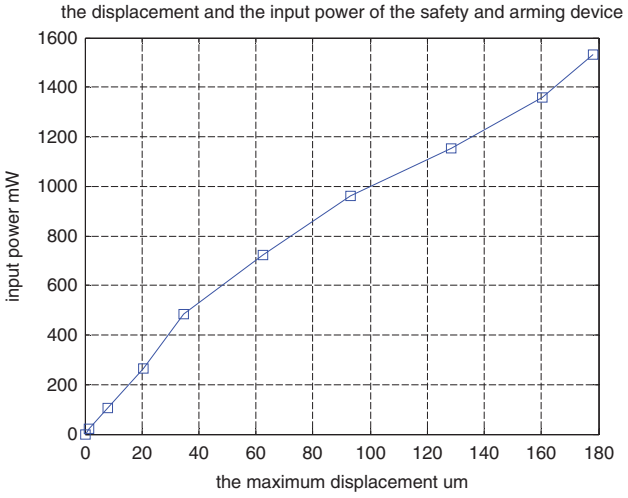

Figure 12: The relationship between the displacement of the whole device and the applied power.

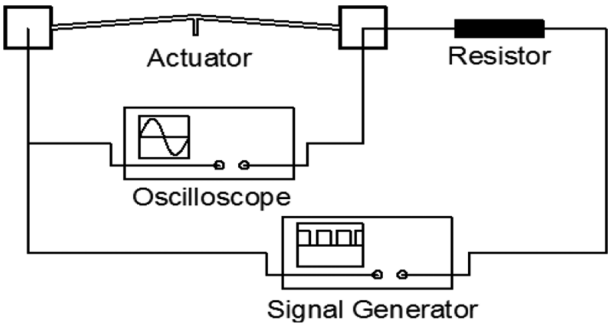

Figure 13: Experimental setup for performance evaluation.

Figure 14: Dynamic characteristic of the whole device.

in applied voltage. Figure 14 shows the dynamic respond of the electro-thermal actuator under the square signal. The response time of the actuator is about 10 ms.

Conclusion

The design, fabrication and characterization of a distinctive electro-thermal MEMS safety-and arming device are presented in this paper. The device is comprised of a V-shape actuator and a micro lever. Under the applied voltage 17 V, the maximum displacement of the device is 178.809 μm, the consuming power is 1.53 W and the respond time is about 10 ms. The chip size is $5 \times 5 \times 0.5$ mm^3, which can be easily integrated with other micro devices.

Funding: The work was supported by the State Key Laboratory for Manufacturing System Open Research Fund (No. sklms2013002).

References

Chiorean, R. S., M. C. Dudescu, M. Pustan, et al. 2014. "Analytical and numerical study on the maximum force developed by a V-beam thermal actuator." *Procedia Technology* 12:359–63.

De Dobbelaere, P., et al. 2002. "Digital MEMS for Optical Switching." *IEEE Communications Magazine*, Vol. 40, Mar 2002.

Donald, R. G., et al. 2001. "MEMS Emergetic Actuator with Integrated Safety and Arming System for a Slapper/EFI Detonator." US Patent 6173650 B1, Jan. 16, 2001.

Dong, Y., et al. 2003. "Modeling of two-hot-arm horizontal thermal actuator." *Journal of Micromechanics and Microengineering* 13:312–22.

Enikov, E. T., S. S. Kedar, and K. V. Lazarov. 2005. "Analytical model for analysis and design of V-shaped thermal microactuators." *Journal of Microelectromechanical System* 14(4):788–798.

Jay, J. K., H. W. Qu, et al. 2011. "Design and Fabrication of Electro-thermally Activated Micro Gripper with Large Tip Opening and Holding Force." In IEEE 2011 Conference.

Lai, Y. J., E. V. Bordatchev, and S. K. Nikumb. 2006. "Performance characterization of in-plane electro-thermally driven linear microactuators." *Journal of Intelligent Material Systems and Structures* 17:919.

Lake, R. A., L. A. Starman, et al. 2010. "Electrothermal Actuators for Integrated MEMS Safe and Arming Devices." In Proceedings of the SEM Annual Conference. June 7–10, 2010 Indianapolis, Indiana USA.

Ostrow II, S. A., R. A. Lake, J. P. Lombardi III, et al. 2012. "Fabrication process comparison and dynamics evaluation of electrothermal actuators for a prototype MEMS safe and arming devices." *Experimental Mechanics* 52:1229–38. DOI 10.1007/s11340-011-9579–8.

Robinson, C. H., R. H. Wood, and T. Q. Hoang. 2005. "Miniature MEMS-Based Electro-Mechanical Safety and Arming Device." US Patent 6964231 B1, Nov. 15, 2005.

Robinson, C. H. 2003. "Microelectromechanical System (MEMS) Safe and Arm Apparatus." US Patent 6568329 B1, May. 27, 2003.

Yang, Y. S., et al. 2009. "A large-displacement thermal actuator designed for MEMS pitch-tunable grating." *Journal of Micromechanics and Microengineering* 19:015001.

Zhang, Y. X., et al. 2006. "Macro-modeling for polysilicon cascaded bent beam electrothermal microactuators." *Sensors and Actuators A* 128:165–75.

Zunino III, J. L., et al. 2008. "Reliability Testing and Analysis of Safing and Arming Devices for Army Fuzes." Proceedings of SPIE 6884:0C1-0C12, 2008.